Vol 16 No 11, November 2007
1009-1963/2007/16(11)/3434-09

Chinese Physics

© 2007 Chin. Phys. Soc.
and IOP Publishing Ltd

Modification to poloidal charge exchange recombination spectroscopy measurement in JT-60U tokamak*

Ding Bo-Jiang(丁伯江)[a)†], Sakamoto Yoshiteru[b)], and Miura Yukitoshi[b)]

[a)] *Institute of Plasma Physics, Chinese Academy of Sciences, Hefei* 230031, *China*
[b)] *Japan Atomic Energy Agency, Naka-machi, Naka-gun, Ibaraki* 311-0193, *Japan*

(Received 20 March 2007; revised manuscript received 21 June 2007)

With consideration of the effects of the atomic process and the sight line direction on the charge exchange recombination spectroscopy (CXRS), a code used to modify the poloidal CXRS measurement on Tokamak-60 Upgrade (JT-60U) in Japan Atomic Energy Research Institute is developed, offering an effective tool to modify the measurement and analyse experimental results further. The results show that the poloidal velocity of ion is overestimated but the ion temperature is underestimated by the poloidal CXRS measurement, and they also indicate that the effect of observation angle on rotation velocity is a dominant one in a core region ($r/a < 0.65$), whereas in an edge region where the sight line is nearly normal to the neutral beam, the observation angle effect is very small. The difference between the modified velocity and the neoclassical velocity is not larger than the error in measurement. The difference inside the internal transport barrier (ITB) region is 2–3 times larger than that outside the ITB region, and it increases when the effect of excited components in neutral beam is taken into account. The radial electric field profile is affected greatly by the poloidal rotation term, which possibly indicates the correlation between the poloidal rotation and the transport barrier formation.

Keywords: atomic process, charge exchange recombination spectroscopy (CXRS), modification, plasma

PACC: 5200, 3270J, 5270

1. Introduction

The shear of radial electric field has been considered to have an important effect on confinement and anomalous transport in plasmas.[1−8] The poloidal plasma rotation velocity is a key ingredient determining a radial electric field. In order to analyse the plasma confinement, it is, of course, very important to acquire an accurate plasma rotation velocity. In JT-60U,[9] this rotation velocity is diagnosed by charge exchange recombination spectroscopy (CXRS)[10] through analysing the impurity ion (C^{5+}) line emission profile. However, the line emission measured by charge exchange reaction (CXR)[11] ($C^{6+}+D^0 \rightarrow C^{5+}+D^+$) cannot reflect the real velocity distribution function of the fully ionized ion (C^{6+}) because of the following effects:[12,13] finite lifetime of the excited states, charge exchange cross section, variation of the ion gyro frequency with charge state ($Z \rightarrow Z-1$), neutral beam non-uniformity and its observation direction. As a consequence, the pseudo velocity is not associated with the real plasma rotation velocity. Just because of the pseudo shift coming from the effects of atomic process and observation angle, in JT-60U tokamak, not the measured poloidal velocity is used to calculate the radial electric field, but the neoclassical velocity. In fact, this is questionable because the difference between the real poloidal velocity and the neoclassical velocity is unknown. Therefore, it is necessary to evaluate the measured line emission with taking into account the above effects, so as to modify the plasma rotation velocity, as well as the ion temperature and the impurity density, and to calculate the radial electric field on the basis of the measured poloidal velocity further.

The effects of gyro motion and finite lifetime on velocity measurements have been considered in Ref.[14], in which a pseudo velocity is produced by the spatial variation of excitations. With the gyro-orbit and the finite lifetime effects on the line shape taken into consideration, the distribution function of ions after undergoing charge exchange has been derived.[12] By integrating the distribution function over the velocity components perpendicular to the sight line, a

*Project supported by the Core University Program between Japan and China and the Scientist Exchange Program in the field of Nuclear Energy Research organized by the Ministry of Education, Culture, Sports, Science and Technology (MEXT) of Japan.

line profile in a particular observation direction can also be obtained.

A corrected velocity can be estimated by using two sets of measurement systems (upper and lower sight lines in a the poloidal plane), such as on Tokamak Fusion Test Reactor (TFTR).[13,15] Such a condition of two-set system is somewhat critical because not all machines can meet this demand. For example, the JT-60U cannot satisfy the condition.

Correction of measured poloidal velocity shift can be made by integrating the distribution function of excited ions described in Ref.[12], in which only a pseudo shifted velocity can be estimated but a modified intensity profile cannot be directly obtained. According to the theory in Ref.[12], in the present work, we develop a modification code to modify the intensity profile, from which the modified plasma poloidal velocity, ion temperature, and the impurity density can be induced.

The remainder of this paper is organized as follows. Derivation of the modified intensity profile is described in Section 2. In Section 3, the modification results and analysis are discussed, including the cross-check of the modification, comparisons of velocities and radial electric fields, and correlation between poloidal rotation velocity and transport barrier. The effect of excited components of neutral beam on the modification is briefly discussed in Section 4. Finally, some conclusions are drawn from the present study in Section 5.

2. Derivation of modified intensity profile

2.1. Line profile determined by the ground ions

We define an orthogonal coordinates of x, y and z, such that v_x, v_y, v_z are along the radial direction, the sight line direction and the magnetic field direction, respectively. The distribution function of ground ions (C^{6+}), F, is assumed to have the Fourier expansion in ψ,

$$F = \sum_{n=-\infty}^{+\infty} F_n \mathrm{e}^{in\psi}, \tag{1}$$

where ψ is the angle measured from the x-axis, so that $v_x = v_\perp \cos\psi$ and $v_y = v_\perp \sin\psi$, with $v_\perp$ being the gyro-velocity in the x–y plane.

After integrating F over the velocity components perpendicular to the sight line ($\mathrm{d}\sigma = \mathrm{d}v_x \mathrm{d}v_z$), the line intensity profile C^{6+} along the sight line direction (v_y) is as follows:[14,16]

$$\begin{aligned} I_y(C^{6+}) &\propto \int F(v)\mathrm{d}v_x\mathrm{d}v_z \\ &\propto \exp\left\{-\frac{M[v_y - (v_{\boldsymbol{E}\times\boldsymbol{B}} + v_{\mathrm{dia}} + v_T)]^2}{2T}\right\}, \end{aligned} \tag{2}$$

where $v_{\boldsymbol{E}\times\boldsymbol{B}}$ is the magnitude of drift velocity caused by $\boldsymbol{E}\times\boldsymbol{B}$, v_{dia} is the diamagnetic drift velocity caused by a pressure gradient, and v_T is the velocity caused by a temperature gradient. Expressions of v_{dia} and v_T are written as

$$v_{\mathrm{dia}} = -\frac{1}{\Omega} \times \frac{T}{M}\left(\frac{1}{n}\frac{\partial n}{\partial x} + \frac{1}{T}\frac{\partial T}{\partial x}\right), \tag{3}$$

$$v_T = -\frac{1}{M\Omega}\left(\frac{M}{2T}v_y^2 - \frac{3}{2}\right)\frac{\partial T}{\partial x}, \tag{4}$$

where Ω is the gyrofrequency of the ground ions.

In a tokamak geometry, there is a tilted angle $\pi/2 - \theta$ between the poloidal direction and the above sight line direction (v_y), where θ is the angle between the poloidal direction and z-axis (magnetic field direction), so we have $\sin\theta = B_{\mathrm{tor}}/B_{\mathrm{total}}$. The intensity profile along the poloidal direction ($v_p = v_y \sin\theta$) is approximately

$$I_p(\mathrm{C}^{6+}) \propto \exp\left\{-\frac{M[v_p - (v_{\boldsymbol{E}\times\boldsymbol{B}} + v_{\mathrm{dia}} + v_T)\sin\theta]^2}{2T}\right\}. \tag{5}$$

Equation (5) can be expanded into

$$\begin{aligned} I_p(\mathrm{C}^{6+}) &\propto \exp\left\{-\frac{M(v_p - v_0)^2 - 2M \times v_T \sin\theta(v_p - v_0) + M(v_T\sin\theta)^2}{2T}\right\} \\ &\propto \exp\left\{-\frac{M(v_p - v_0)^2}{2T}\right\} \times \exp\left\{\frac{Mv_T(v_p - v_0)}{T}\right\} \times \exp\left\{\frac{M(v_T\sin\theta)^2}{2T}\right\}, \end{aligned} \tag{6}$$

from which a shifted velocity along the poloidal direction can be obtained by fitting the line profile $\exp\left\{-\frac{M(\upsilon_p-\upsilon_0)^2}{2T}\right\}$, where $\upsilon_0=(\upsilon_{\boldsymbol{E}\times\boldsymbol{B}}+\upsilon_{\rm dia})\sin\theta$ represents the drifting velocity along the poloidal direction.

2.2. Measured emission profile

With considering the CXRS process, the emission from a unit volume of plasma is proportional to the product of the beam neutral density, the impurity ion density, and the charge exchange rate coefficient

$$E\propto<\sigma\upsilon>, \tag{7}$$

$$<\sigma\upsilon>=\int {\rm d}\upsilon^3\sigma(|\boldsymbol{\upsilon}-\boldsymbol{\upsilon}_{\rm beam}|)\,|\boldsymbol{\upsilon}-\boldsymbol{\upsilon}_{\rm beam}|\,F(\boldsymbol{\upsilon}). \tag{8}$$

The measured intensity profile is dependent on the emission rate

$$Q(\upsilon_{\rm col})=\sigma(|\boldsymbol{\upsilon}-\boldsymbol{\upsilon}_{\rm beam}|)\,|\boldsymbol{\upsilon}-\boldsymbol{\upsilon}_{\rm beam}|\,, \tag{9}$$

where $\boldsymbol{\upsilon}$ and $\boldsymbol{\upsilon}_{\rm beam}$ are the ion velocity and the beam velocity, respectively.

With considering the following effects:
(1) the finite lifetime of the excited states, (2) velocity dependence of charge exchange reactivity,(3) variation of the ion gryofrequency with charge state ($Z\rightarrow Z-1$), and (4) the direction of observed sight line, the distribution function (f) of the excited ions (C^{5+}), determined by the kinetic equation for the excited ions which are formed by CXR, has the following form:[12]

$$\begin{aligned} f \;=\; & \frac{F_0}{\nu}\left[\nu_{\rm CX}+\tilde{\nu}_{\rm CX}\frac{\upsilon_z\cos\theta_{\rm H}-u\sin\theta_{\rm H}\sin\psi_{\rm H}}{\upsilon_{\rm H}}\right] \\ & +\frac{1}{\omega^2+\nu^2}\left\{-\frac{\partial F_0}{\partial x}\frac{\partial\nu_{\rm CX}}{\partial x}\left[\nu\left(\Omega-\omega\right)\upsilon_x+\left(\omega\Omega+\nu^2\right)\upsilon_y\right]\right. \\ & \left.+\frac{F_0\tilde{\nu}_{\rm CX}}{\upsilon_{\rm H}}\sin\theta_{\rm H}\left[\left(\nu\cos\psi_{\rm H}-\omega\sin\psi_{\rm H}\right)\upsilon_x+\left(\nu\sin\psi_{\rm H}+\omega\cos\psi_{\rm H}\right)\upsilon_y\right]\right\}, \end{aligned} \tag{10}$$

where u is the magnitude of the drift velocity caused by $\boldsymbol{E}\times\boldsymbol{B}$; $\nu_{\rm CX}$ and $\tilde{\nu}_{\rm CX}$, defined in Ref.[12], are the constants of the dimension of frequency characterizing the charge exchange rate; $\theta_{\rm H}$ is the polar angle of the neutral beam measured from the z-axis; $\psi_{\rm H}$ is the azimuthal angle of the neutral beam measured from the x-axis; $\upsilon_{\rm H}$ is the mean-square velocity of the neutral beam; ω is the gyrofrequency of the excited ions; $\nu=1/\tau$.

We characterize the direction of the sight line by the polar coordinate (θ_0, ψ_0), with the polar angle θ_0 measured from the z-axis and the azimuthal angle ψ_0 measured from the x-axis. In the CXRS measurement, the sight line is usually in the poloidal plane. Since the poloidal magnetic field ($B_{\rm pol}$) is much smaller than the toroidal magnetic field ($B_{\rm tor}$) in JT-60U (usually, $B_{\rm pol}/B_{\rm tor}<0.1$), the magnetic field is nearly perpendicular to the poloidal plane. Therefore, we have approximately $\theta_0\sim\theta$, which is the angle between the poloidal direction and the magnetic field direction. In addition, the presence of ψ_0 suggests that the sight line is not along the poloidal direction, but in the direction of $\upsilon_{\rm obs}$ which is indicated in Fig.1 showing the poloidal plane ($\upsilon_{\rm obs}=\upsilon_p\sin\psi_0+\upsilon_x\cos\psi_0$, where ψ_0 is also called the observation angle measured from the radial x-axis). As a result, the measured shift is not

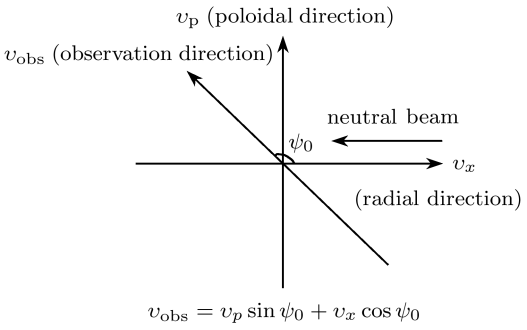


Fig.1. Sight line in the poloidal plane.

a pure poloidal rotation velocity. A line profile in the observation direction, obtained by integrating f over the velocity components particular to the of sight line, is

$$I(\text{obs}) \propto \int Q(v_{\text{col}}) f(v) \mathrm{d}\sigma, \tag{11}$$

i.e.

$$\begin{aligned} I(\text{obs}) &\propto \int f(v)\mathrm{d}\sigma \\ &\propto \exp\left\{-\frac{M(v_{\text{obs}} - v_{\boldsymbol{E}\times\boldsymbol{B}}\sin\theta_0\sin\psi_0 - u_1 - u_2 - u_3 - u_4)^2}{2T}\right\} \propto \exp\left\{-\frac{M(v_{\text{obs}} - v_{\text{measure}})^2}{2T}\right\} \\ &\propto \exp\left\{-\frac{M(v_p\sin\psi_0 - v_x\cos\psi_0 - v_{\text{measure}})^2}{2T}\right\} \\ &\propto \exp\left\{-\frac{M[(v_p\sin\psi_0 - v_{\text{measure}})^2 + v_x^2\cos^2\psi_0 - 2\times v_x\cos\psi_0\times(v_p\sin\psi_0 - v_{\text{measure}})]}{2T}\right\} \\ &\propto A\exp\left\{-\frac{M(v_p\sin\psi_0 - v_{\text{measure}})^2}{2T}\right\}, \end{aligned} \tag{12}$$

$$\left(A = \exp\left\{-\frac{M(v_x^2\cos^2\psi_0 - 2\times v_x\cos\psi_0\times(v_p\sin\psi_0 - v_{\text{measure}}))}{2T}\right\}\right), \tag{13}$$

where v_{measure} is the raw shifted velocity measured by CXRS, u_1, u_2, u_3, and u_4 are defined as those in Ref.[12].

2.3. Modification of the measured intensity profile

Equation (12) can be written in the following form:

$$\begin{aligned} I(\text{obs}) &\propto A\exp\left\{-\frac{M\left[v_p - v_{\boldsymbol{E}\times\boldsymbol{B}}\sin\theta_0 - \dfrac{(u_1+u_2+u_3+u_4)}{\sin\psi_0}\right]^2\sin^2\psi_0}{2T}\right\}, \\ I(\text{obs}) &\propto A\exp\left\{-\frac{M\left[v_p - (v_{\boldsymbol{E}\times\boldsymbol{B}} + v_{\text{dia}})\sin\theta_0 - \dfrac{(u_1'+u_2+u_3+u_4)}{\sin\psi_0}\right]^2}{2T\sin^2\psi_0}\right\}, \end{aligned} \tag{14}$$

where $u_1' = u_1 - v_{\text{dia}}\sin\theta_0\sin\psi_0$. Since $\theta_0 \sim \theta$, we have $v_0 = (v_{\boldsymbol{E}\times\boldsymbol{B}} + v_{\text{dia}})\sin\theta_0$. Taking $v_1 = (u_1' + u_2 + u_3 + u_4)/\sin\psi_0$, we have

$$I(\text{obs}) \propto \exp\left\{-\frac{M[(v_p - v_0) - v_1]^2}{2T/\sin^2\psi_0}\right\} A = A\exp\left\{-\frac{M[(v_p - v_0)^2 + v_1^2 - 2(v_p - v_0)v_1]}{2T/\sin^2\psi_0}\right\}, \tag{15}$$

where v_0 and v_1 are small shift values compared with the ion thermal velocity ($< 10\%$ in JT-60U), so $\dfrac{Mv_1^2}{2T}$ and $\dfrac{Mv_0v_1}{2T}$ are the terms of the second-order smallness and can be neglected. Thus, Eq.(15) is expressed as

$$I(\text{obs}) \propto A\exp\left\{-\frac{M(v_p - v_0)^2}{2T/\sin^2\psi_0}\right\}\exp\left\{\frac{Mv_pv_1}{T/\sin^2\psi_0}\right\}. \tag{16}$$

Integrating the above equation over the observation direction yields

$$\int I(\text{obs})\mathrm{d}v_{\text{obs}} \propto \exp\left\{-\frac{M(v_p - v_0)^2}{2T/\sin^2\psi_0}\right\}\exp\left\{\frac{Mv_pv_1}{T/\sin^2\psi_0}\right\}\int A\mathrm{d}v_{\text{obs}}, \tag{17}$$

$$\exp\left\{-\frac{M(v_p - v_0)^2}{2T/\sin^2\psi_0}\right\} \propto \int I(\text{obs})\mathrm{dv_{obs}})/\exp\left\{\frac{Mv_pv_1}{T/\sin^2\psi_0}\right\} \Big/ \left(\int A\mathrm{d}v_{\text{obs}}\right). \tag{18}$$

Note that the term on the left-hand side in Eq.(18) is just corresponding to the impurity ion (C^{6+}) line profile obtained from Eq.(6) expressed as $\exp\left\{-\frac{M(\upsilon_p-\upsilon_0)^2}{2T'}\right\}$, where T' is the modified ion temperature. By modifying the measurement by using Eq.(18), a shifted velocity and temperature can be induced.

3. Modification results and analysis

In the poloidal CXRS measurement on JT-60U, the neutral beam is injected in a direction opposite to the radial direction (see Fig.1). In the modification, the C VI ($n = 8 \rightarrow 7$) transition is used and the corresponding wavelength is $\lambda = 529.05\,\text{nm}$, which is used in the CXRS measurement in JT-60U. Also, three components of neutral beam at the full (85 keV), half and third energies account for 50%, 27%, and 23% of components of the beam, respectively. The energy-dependent emission rate is cited from Ref.[17] and the lifetime is taken as 1.1ns obtained in experiments.[13] The computed line profiles include summations over the three components.

3.1. Cross-check for the modifications

With the modification expressed by Eq.(18), assuming a JT-60U plasma (shot 36479 ($t = 6.0\,\text{s}$)),[10] to have a Maxwellian velocity distribution with $T_\text{i} = 7.601\,\text{keV}$ and $\upsilon_\text{measure} = -40206\,\text{m/s}$ (here, the sign '–' means the diamagnetic drift direction of ion) measured by the poloidal CXRS at an observation angle $\psi_0 = 115°$, the relative intensity profiles with and without taking into account the effect of sight line are displayed in Fig.2. The figure shows that the spectrum changes very little without considering the observation angle effect (i.e. $\psi_0 = 90°$), and that the spectrum, the resulting ion temperature, and rotation velocity are modified greatly when the observation angle effect is taken into account (at the point, $\psi_0 = 115°$). It is clearly seen that in the case of considering the observation angle effect, the absolute value of modified velocity is much smaller than the original measurement and the ion temperature is higher than the measurement, indicating that the poloidal velocity is overestimated and ion temperature is underestimated by the poloidal CXRS measurement. When the observation angle effect is ignored, i.e. the sight line is normal to the neutral beam, the velocity difference becomes small and little change in ion temperature occurs within the error bar. The modification has a similar change tendency to the result (shown in Fig.3) obtained by the simulation introduced in Ref.[18], indicating the reliability of the modification results. The poloidal rotation velocity profiles with and without modifications are shown in Fig.4, separately indicating that the effect of observation angle on rotation velocity is much larger than the other effects (e.g. emission rate and life time) in a region of $r/a < 0.65$, whereas outside this region where the sight line is nearly normal to neutral beam, the observation angle effect is very small.

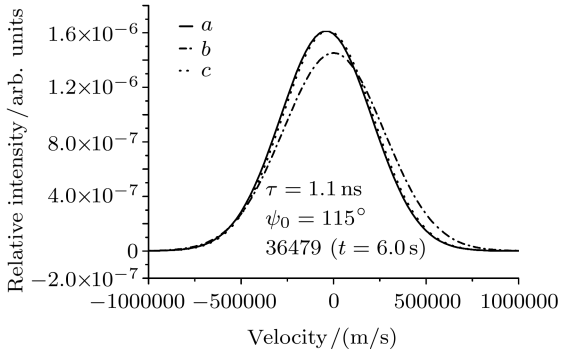


Fig.2. Relative intensity profiles before and after modifications. correction 1 — with effects of lifetime and observation angle. correction 2 — with lifetime effect but without observation angle effect. *a* before correction ($V^\text{peak} = -40246\,\text{m/s}, T_\text{i} = 7.601\,\text{keV}$); *b* correction 1 ($V^\text{peak} = -372\,\text{m/s}, T_\text{i} = 9.256\,\text{keV}$); *c* correction 2 ($V^\text{peak} = -30577\,\text{m/s}, T_\text{i} = 7.59\,\text{keV}$).

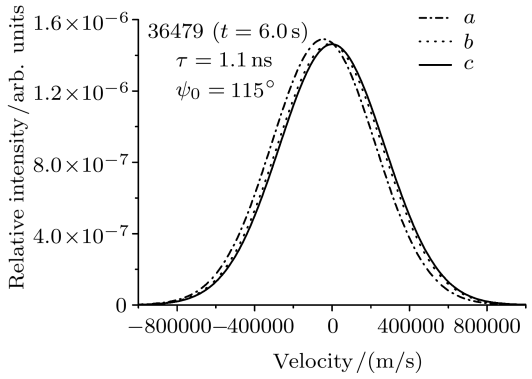


Fig.3. Simulated relative intensity profiles before and after CXRS processes. *a* with observation angle ($V^\text{peak} = -45093\,\text{m/s}, T_\text{i} = 8.91\,\text{keV}$); *b* without observation angle ($V^\text{peak} = -12014\,\text{m/s}, T_\text{i} = 9.23\,\text{keV}$); *c* assumed profile ($V^\text{peak} = 0, T_\text{i} = 9.25\,\text{keV}$).

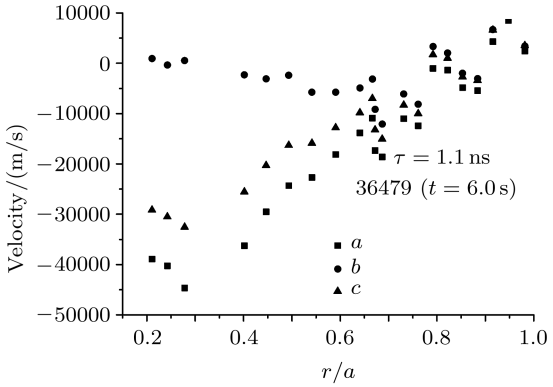


Fig.4. Poloidal rotation velocity profiles before and after modifications. *a* before correction; *b* correction 1 (with effect of lifetime and observation angle); *c* correction 2 (with lifetime effect but without observation angle effect).

For the JT-60U plasma profile (shot 36479 (t = 6.0 s)), the profiles of pseudo velocity, defined as the difference between original measurement and modified result ($\Delta v = v_{\rm measure} - v_{\rm correction}$), are compared with the simulated velocity shifts[18] that are not associated with the poloidal rotation, as shown in Fig.5. It is seen that within the measurement error ($\sim 10^4$ m/s),[10] the two results are almost in agreement with each other no matter whether the observation angle is taken into account or not.

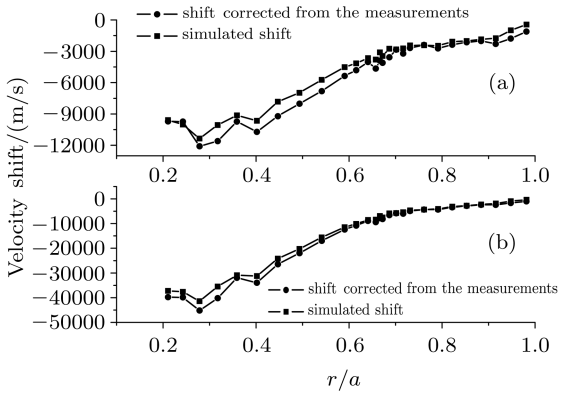


Fig.5. Comparison between modified and simulated velocity profiles (The shift corrected from the measurement is defined as $\Delta v = v_{\rm measure} - v_{\rm correction}$) (a) with lifetime effect but without observation angle effect (b) with effects of lifetime and observation angle.

The comparisons all show that the modified results are almost reliable, so that it could be used to modify the poloidal rotation velocity, hence to evaluate the radial electric field (E_r) and analyse the improvement on plasma parameters.

Though, for the ion temperature case, there exist some quantitative differences between the modification (Fig.2) and the simulation (Fig.3), the comparisons between experimental data support the validation of modification in some degree. The ion temperature profiles (shot 36479 (t = 6.0 s)), diagnosed by the poloidal CXRS, before and after modifications are shown in Fig.6, in which the ion temperature profile measured by the toroidal CXRS is also displayed. It is observed that the modified ion temperature from the poloidal CXRS measurement is nearly equal to the toroidal measurement within the error-bar, which possibly suggests the reliability of the modification experimentally.

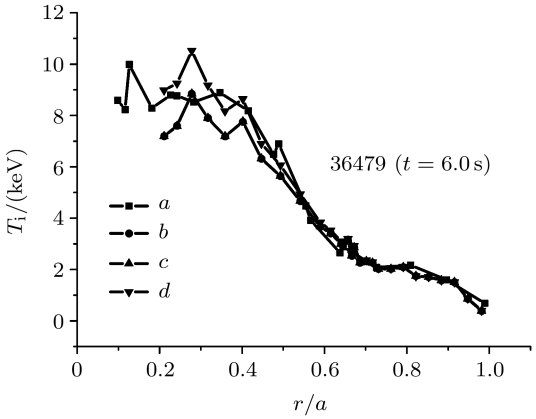


Fig.6. Comparison between ion temperatures from poloidal and toroidal CXRS measurements. *a* toroidal measurement; *b* poloidal measurement; *c* correction without observation angle effect; *d* correction with observation angle effect.

In addition, as is in agreement with the simulation results shown in Ref.[18], it is seen from Fig.4 that in an edge region there is little difference between the measurement and the modification, which is because in that region the ion temperature is low and the sight line is nearly perpendicular to the neutral beam. The result indicates that the measured spectrum in this region can be directly used to calculate the radial electric field and no correction is needed on the condition of the reliability of the measurement system.

3.2. Poloidal rotation velocities and radial electric fields

For a discharge of 36486 (t = 5.9 s)[19] with ITB, a modified velocity profile evaluated according to the measurement is displayed in Fig.7, in which also shown are profiles including the original measurement and the neoclassical poloidal velocity. It

is shown that though the modified result is a little larger than the neoclassical value and the difference ($\sim$3000 m/s) is much smaller than the measurement error ($\sim 10^4$m/s)[10] outside the ITB region, the velocity discrepancy increases and the difference is of almost the same order of magnitude as the measurement error inside the ITB region. The difference inside the ITB region is $2 \sim 3$ times larger than that outside the ITB region. The radial electric field profile could be different due to the discrepancy in the velocity profile inside the ITB region.

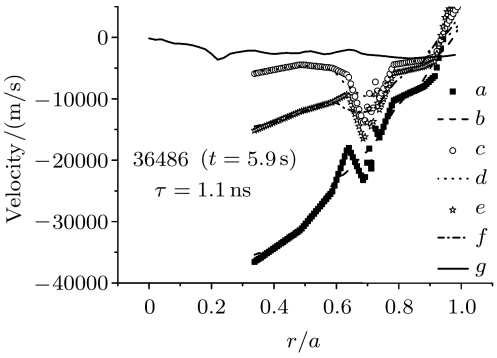


Fig.7. Comparison among originally measured, modified and neoclassical velocity (the dots denote the measurements and modifications, the 'smoothed' means averaging the dots into a smoothed line). Modification 1: without considering the charge exchange cross section in excited state. Modification 2: considering the charge exchange cross section in excited state. *a* original measurement; *b* smoothed measurement; *c* modification 1; *d* smoothed modification 1; *e* modification 2; *f* smoothed modification 2; *g* neoclassical velocity.

By using the balance in radial force, a radial electric field (E_r) can be calculated from the equation

$$E_r = \frac{1}{eZn}\frac{\partial p}{\partial r} + v_\varphi B_\theta - v_\theta B_\varphi, \tag{19}$$

where e, Z, n, p are the electric charge, nuclear charge of impurity ion, ion density, and ion pressure, respectively, and v_φ is the impurity ion toroidal rotation velocity, v_θ the poloidal rotation velocity, B_φ the toroidal magnetic field, and B_θ the poloidal magnetic field. By substituting v_θ in Eq.(19) with the modified velocity and the neoclassical value, the E_r profiles, together with different E_r components of pressure gradient $\left(\frac{1}{eZn}\frac{\partial p}{\partial r}\right)$, poloidal rotation ($-v_\theta B_\varphi$), and toroidal rotation ($v_\varphi B_\theta$) are displayed in Fig.8. Though the differences between the modified and the neoclassical velocities is within the measurement error-bar, the radial electric fields, particularly E_r shear, evaluated with the modified velocity are affected by the poloidal rotation term. No matter whether the modified velocity or the neoclassical value is used, the peak positions of E_r are almost consistent. It seems that the modification increases the shear of E_r because the maximum of poloidal rotation term is close to the ITB foot, thus deepening the E_r well relatively. Whether it results in or from the formation of ITB is not very clear, which needs further studying.

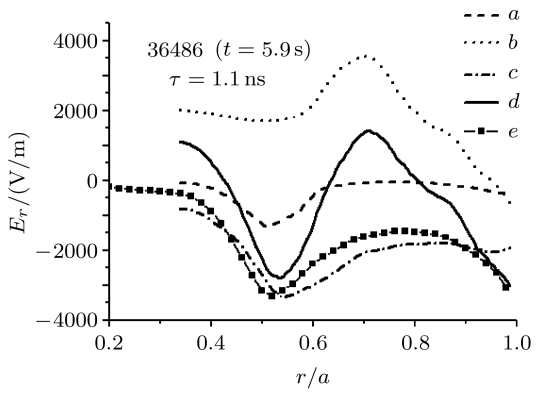


Fig.8. Radial electric field (E_r) profiles, calculated using modified and neoclassical velocity, together with different E_r components of pressure gradient $\left(\frac{1}{eZn}\frac{\partial p}{\partial r}\right)$, and poloidal rotation ($-v_\theta B_\varphi$), and toroidal rotation ($v_\varphi B_\theta$). *a* pressure gradient term; *b* poloidal rotation term; *c* toroidal rotation term; *d* E_r with modified velocity; *e* E_r with neoclassical velocity.

The electric fields calculated from Eq.(19), separately, with the originally measured, modified, and neoclassical poloidal velocity are compared in Fig.9. It is obvious that the electric field calculated by using the original measurement is far different from those obtained by using the modified velocity and neoclassical value. At the same time, another radial electric field profile calculated by using modified velocity at $\tau = 0.59$ ns is also shown in Fig.9, indicating that the radial electric field is affected somewhat by the τ value, especially in the core region where the ion temperature and the observation angle are large. This indicates that a reliable lifetime is necessary to acquire a reliable calibration.

For the edge transport barrier (ETB) case, a high confinement (H-mode) plasma (shot 24573 $t = 6.35$ s)[20] is analysed as follows. Figure 10 (a) shows the edge pressure ($n_e T_i$) profile, indicating the existence of H-mode pedestal near $r/a \sim 0.9$. Figure 10(b) shows the corresponding poloidal velocity profile. Shown in Fig.11 are three radial electric field com-

ponents, i.e. poloidal rotation term $(-v_\theta B_\varphi)$, summation of pressure gradient and toroidal rotation term $\left(\frac{1}{eZn}\frac{\partial p}{\partial r}+v_\varphi B_\theta\right)$, and summation of pressure gradient term, toroidal rotation term and poloidal rotation term $\left(\frac{1}{eZn}\frac{\partial p}{\partial r}+v_\varphi B_\theta - v_\theta B_\varphi\right)$, i.e. total E_r. This figure indicates that the radial electric field profile is greatly modified by the poloidal rotation term, especially in a transport barrier region the shear of E_r is increased dramatically due to the poloidal rotation at a larger poloidal velocity localized near the ETB shoulder, which possibly indicates the correlation between the poloidal rotation and the pedestal structure.

Of course, the obtained relationship between the poloidal rotation velocity and the transport barrier is preliminary only, for the data is not enough. Further study is under way in detail, especially on the analysis of the influence of poloidal rotation on the edge transport. Because the above results indicate that the modification to measurement is not necessary in the edge region, the uncertainty of lifetime can be avoided.

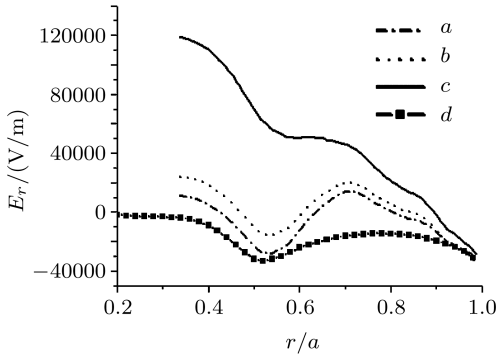


Fig.9. Comparisons among the radial electric field obtained with originally measured, modified, and neoclassical poloidal velocity. *a* with modified velocity ($\tau = 1.1$ ns); *b* with modified velocity ($\tau = 0.59$ ns); *c* with unmodified velocity; *d* with neoclassical velocity.

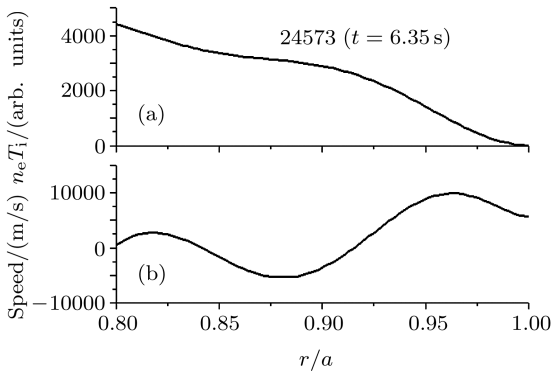


Fig.10. (a) Edge pressure ($n_\mathrm{e} \times T_\mathrm{i}$) profile for an H-mode plasma (24573); (b) Poloidal velocity profile (24573).

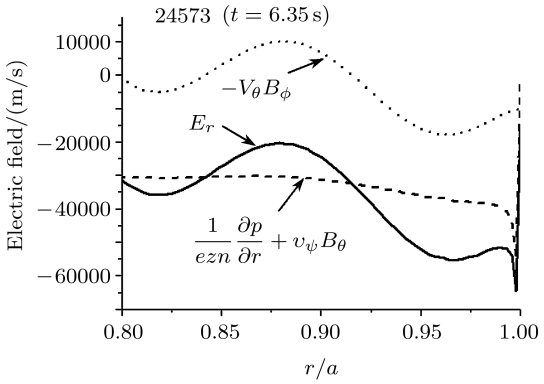


Fig.11. Three component of radial electric field: poloidal rotation term $(-v_\theta B_\varphi)$, summation of pressure gradient and toroidal rotation term $\left(\frac{1}{eZn}\frac{\partial p}{\partial r}+v_\varphi B_\theta\right)$, and total radial electric field $\left(E_r = \frac{1}{eZn}\frac{\partial p}{\partial r}+v_\varphi B_\theta - v_\theta B_\varphi\right)$.

4. Discussion

Here we discuss the effect of excited components of neutral beam on the modification. No error analysis is made in the above modification, for it is very difficult to make the error analysis in such a modification, especially due to the uncertainties in the atomic physics cross section. In the above modification, the effect of excited components of neutral beam is not taken into account in considering the charge exchange emission rate and observation angle effects. The results show that there is no obvious difference between the inferred poloidal velocity (modification 1 in Fig.7) and the neoclassical velocity, especially outside the ITB region. In fact, the cross section for the $n = 2$ excited neutrals in the beam is two orders of magnitude larger than that for the neutrals in a ground state at lower energies, i.e. half and third energies.[21,22] Previous result[23] shows that although the fraction of neutrals in an excited state is typically less than 1%, the overall effect on the apparent velocity is significant due to the large cross section. Using the charge exchange cross section, interpolated from the Atomic Data and Analysis Structure (ADAS) database, with considering the effect of excited beam neutrals whose component fraction is 0.3%, the modified poloidal velocity profile (modification 2) is also displayed in Fig.7. It is seen that the modified velocity increases, as a result, the difference between the inferred poloidal velocity and the neoclassical velocity increases. The difference between the modified and the neoclassical velocities is greatly affected by the excited components of the

neutral beam, especially in the core region where the temperature is high. Therefore, it is necessary to obtain an accurate component of the $n = 2$ excited neutrals of the beam so as to obtain a reliable poloidal rotation velocity.

5. Conclusions

With taking into account the effects of the atomic process and the sight line direction in the CXRS process, a code used to modify poloidal CXRS measurement on JT-60U is developed, offering an effective tool to modify the measurement and to analyse experimental results further. After making the modification, the results indicate that poloidal velocity is overestimated but the ion temperature is underestimated by the poloidal CXRS measurement. The effect of observation angle on rotation velocity is much larger than the other effects (e.g. emission rate and life time) in the core region, whereas in the edge region where the sight line is nearly normal to neutral beam, the observation angle effect is very small. All of these results are nearly in agreement with the simulated results, indicating the reliability of the modification. The difference between the modified velocity and the neoclassical velocity is not larger than the measurement error. The difference inside the ITB region is $2 \sim 3$ times larger than that outside the ITB region. Such a difference increases when the effect of excited neutrals of the beam is taken into account.

It seems that there exists a correlation between poloidal velocity and transport barrier. The radial electric field profile is greatly modified by the poloidal rotation term, which possibly indicates the correlation between the poloidal rotation and the pedestal structure.

Acknowledgments

Ding B J would like to thank Drs H. Kubo, H. Shirai, S. Ide, S. Higashijima and Ms. H. Tsurumi for useful discussions and warm help during his stay at the Japan Atomic Energy Agency (JAEA). Also, he would like to thank Dr M. von Hellermann for his kind help in calculating the charge exchange cross section.

References

[1] Itoh K and Itoh S 1996 *Plasma Phys. Control. Fusion* **38** 1

[2] Shirai H, Kikuchi M, Takizuka K, Fujita T, Koide Y, Sakamoto Y, Naito O, Hatae T, Isayama A, Kamada Y and Azumi M 2000 *Plasma Phys. Control. Fusion* **42** A109

[3] Shirai H, Kikuchi M, Takizuka T, Fujita T, Koide Y, Rewoldt G, Mikkelsen D, Budny R, Tang W, Kishimoto Y, Kamada Y, Oikawa T, Naito O, Fukuda T, Isei N, Kawano Y, Azumi M and JT-60 Team 1999 *Nucl. Fusion* **39** 1713

[4] Boedo J J, Gray D, Jachmich S, Jachmich S, Conn R, Terry G P, Tynan G, Van Oost G, Weynants R R and TEXTOR Team 2000 *Nucl. Fusion* **40** 1397

[5] Terry P W 2000 *Rev. Mod. Phys.* **71** 109

[6] Yoshizawa A, Itoh S and Itoh K 2003 *Plasma and Fluid Turbulence Theory and Modelling* (London: The Institute of Physics)

[7] Waltz R E 1994 *Phys. Plasma* **1** 2229

[8] Waltz R E, Kerbel G D, Milovich J and Hammett G W 1995 *Phys. Plasma* **2** 2408

[9] Ninomiya H and the JT-60U team 1992 *Phys. Fluids* B **4** 2070

[10] Koide Y, Sakasai A, Sakamoto Y, Kubo H and Sugie T 2001 *Rev. Sci. Instru.* **72** 119

[11] Isler R C 1977 *Phys. Rev. Lett.* **38** 1359

[12] Ryutov D D 2000 *Phys. Plasmas* **7** 1315

[13] Bell R E and Synakowski E J 2000 *Atomic Processes in Plasmas: Twelfth Topical Conf.* (American Institute of Physics) **547** 39

[14] Field A R, Fussmann G, Hofmann J V and the ASDEX Team 1992 *Nucl. Fusion* **32** 1191

[15] Bell R E, Dudek L E, Grek B, Johnson D W and Palladino R W 1999 *Rev. Sci. Instru.* **70** 821

[16] Hinton F L 1983 *Handbook of Plasmas Physics* Vol. 1, (Amsterdam: North-Holland) p177

[17] Von Hellermann M, Bregere P, Frieling J, König R, Mandl W, Maas A and Summers H P 1995 *Plasma Phys. Control. Fusion* **37** 71

[18] Ding B J, Sakamoto Y and Miura Y 2005 *Plasma Phys. Control. Fusion* **47** 789

[19] Sakamoto Y, Kamada Y, Ide S, Fujita T, Shirai H, Takizuka T, Koide Y, Fukuda T, Oikawa T, Suzuki T, Shinohara K, Yoshino R and JT-60 Team 2001 *Nucl. Fusion* **41** 865

[20] Kamada Y, Fujita T, Ishida S *et al* 2002 *Fusion Science and Technology* **42** Sep./Nov. 185

[21] Hoekstra R, Anderson H, Bliek F W, Von Hellermann M, Maggi C F, Olson R E and Summers H P 1998 *Plasma Phys. Control. Fusion* **40** 1541

[22] Isler R C and Olson R E 1988 *Phys. Rev.* A **37** 3399

[23] Solomon W M, Burrell K H and Andre R 2006 *Phys. Plasmas* **13** 056116